EFFECTS OF BEAM BAR BOND AND COLUMN AXIAL LOAD ON SHEAR STRENGTH IN REINFORCED CONCRETE INTERIOR BEAM-COLUMN JOINTS

Shinji MORITA*1, Kazuhiro KITAYAMA*2, Akio KOYAMA*3 and Tomotaka HOSONO*4

ABSTRACT

The influences of a column axial load and a beam bar bond within a joint on the shear strength in reinforced concrete interior beam-column joints were studied. The decrease in the lever arm length at a beam critical section, which was caused by the beam bar bond deterioration within a joint, resulted in the decay of the story shear. The compressive collapse of the diagonal concrete strut developed in the joint panel. The diagonal joint shear however could be carried by the surrounding concrete of the diagonal strut failed by the compression.

KEYWORDS : beam-column joint, beam bar bond deterioration, column axial load, story shear, joint shear

1. INTRODUCTION

Many diagonal shear cracks and the concrete spalling-off are observed in a beam-column joint panel of reinforced concrete buildings subjected to severe earthquake motion. The joint failure such as this had been considered to be caused by a joint shear. Shiohara[1] proposed however that the joint does not fail in a shear, but fails by the increase in the flexural compression at the beam critical section caused by the bond deterioration along beam bars within a joint. Therefore the failure mechanism of an interior beam-column joint was investigated by the tests using six plane cruciform subassemblage specimens.

2. OUTLINE OF TEST

2.1 SPECIMENS

Properties of specimens are shown in Table 1. Section dimensions and reinforcement details are shown in Fig.1. The six interior beam-column joint specimens with one-half scale were tested. Section dimensions and the specified concrete strength (18 MPa) were common for all specimens. The

Table 1 Properties of specimens

Specimens	No. 1	No. 2	No. 3	No. 4	No. 5	No. 6
Column axial load (kN)	C +833	T -833	V ±833	C +833	C +833	T -833
ratio	0.33	-0.33	±0.33	0.32	0.33	-0.33
Beam bar	Top & bottom : 4-D25				Top&bottom:7-D16	
Joint hoops	2-D10@90 3 sets p_{wj}=0.45 %				2-D10@60 3sets p_{wj}=0.57 %	
Spiral steel	none			exist	none	
Common	Specified concrete strength F_c=18 MPa					

C:constant in compression, T:constant in tension, V:varying load

*1 Graduate School of Engineering, Tokyo Metropolitan University, M. Eng.
*2 Associate Professor, Graduate School of Engineering, Tokyo Metropolitan University, Dr. Eng.
*3 Assistant Professor, Dept. of Architecture, Faculty of Science & Technology, Meiji University, Dr. Eng.
*4 Graduate School of Engineering, Tokyo Metropolitan University.

column axial load and the beam bar diameter were chosen as the test parameters. The column axial load was as follows; the constant compressive load of +833 kN, the constant tensile load of −833 kN and the varying load from −833 kN to +833 kN. The beam bar diameter of D16 or D25 was used. The beam longitudinal bars were reinforced by the spiral steel of D3 within both a joint and beam hinge regions in Specimen No.4. The joint lateral reinforcement was 3 sets of 2-D10 for all specimens. Properties of the steel and the concrete are shown in Table 2 and 3.

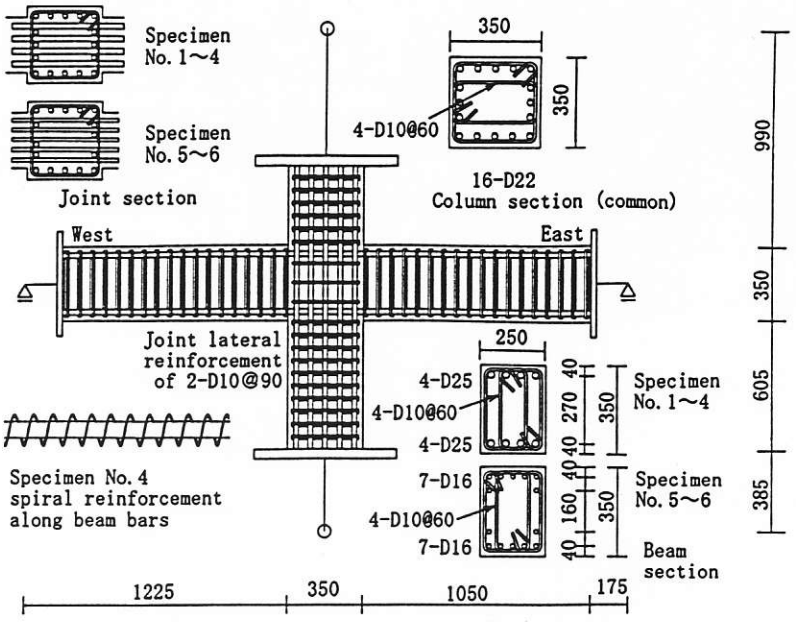

Fig. 1 Section dimensions and reinforcement details

Table 2 Properties of steel bar

diameter	Yeild stress σ_y(MPa)	Tensile strength σ_t(MPa)	Elongation ε_u(%)	Young's Modulus E_s(GPa)
D3	305	402	40.2	128
D10	377	643	14.2	181
D16	508	709	16.5	194
D22	548	739	15.1	196
D25	511	668	16.8	194

E_s : Young's Modulus was obtained by tensile test of steel bar

Table 3 Properties of concrete

Specimens	Compressive strength σ_B(MPa)	Strain at σ_B ε_c(%)	Tensile strength σ_t(MPa)	Young's Modulus E_c(GPa)
No. 1	22.1	0.248	1.75	19.5
No. 2	22.0	0.226	2.28	20.9
No. 3	21.5	0.241	1.71	17.8
No. 4	22.5	0.221	1.59	19.0
No. 5	21.6	0.217	1.71	20.0
No. 6	21.7	0.221	1.88	18.9

E_c: Secant modulus at $1/4\sigma_B$

2.2 LOADING METHOD

The beam ends were supported by horizontal rollers, while the bottom of the column was supported by a mechanical hinge. The reversed horizontal load and the column axial load were applied at the top of the column. The column axial load was controlled by the load, and a lateral force was controlled by the story drift angle θ for 1 cycle of 1/400 radian, 2 cycles of 1/200, 1/100 and 1/50 radian, 1 cycle of 1/33 radian and to the end after 2 cycles of 1/25 radian. The story drift angle or the column axial load was kept constant while the other was changed in Specimen No.3 as shown in Fig.2.

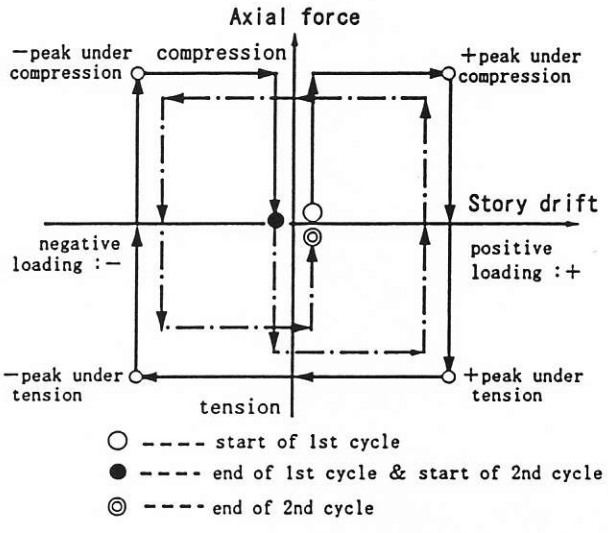

Fig. 2 Loading path for Specimen No. 3

2.3 INSTRUMENTATION

A lateral force applied to the top of a column, the column axial load and the shear forces of both

beam ends were measured by load-cells. A story drift, deflections of both beams and the upper and lower column, local displacements of the joint panel and the slip of the beam bars at the center of a beam-column joint were measured by displacement transducers. The strains of beam bars, column bars and the joint lateral reinforcement were measured by strain gauges.

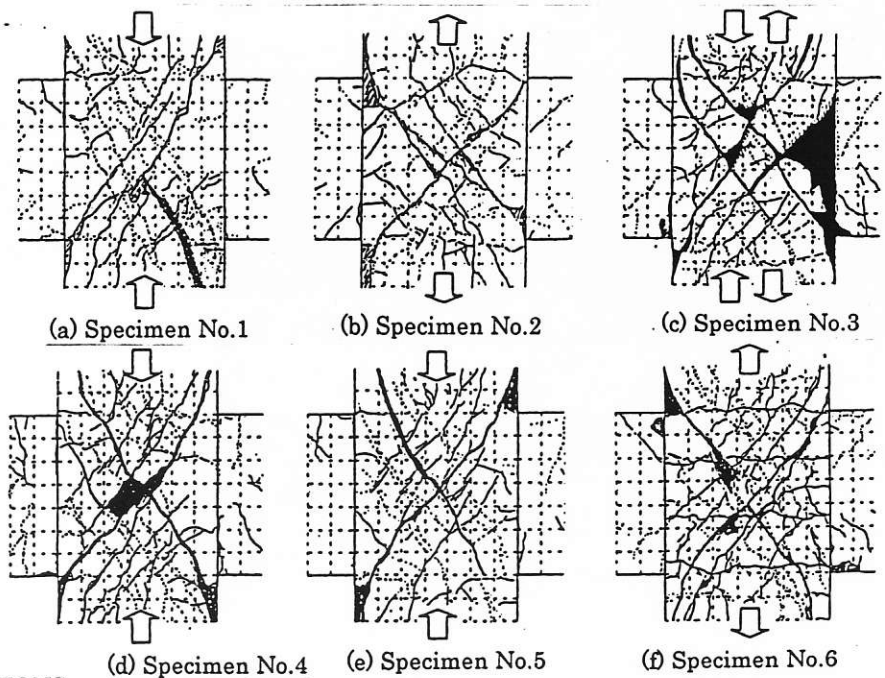

Fig. 3 Crack patterns

3. TEST RESULTS

3.1 GENERAL OBSERVATIONS

The crack patterns after the story drift angle of 1/25 radian are shown in Fig.3. The diagonal shear cracks occurred in the joint panel for all specimens. The diagonal crack angle to a beam axis of the specimens subjected to the constant column axial load in compression somewhat stood up compared with the specimens subjected to the constant column axial load in tension. The concrete spalling-off was observed in

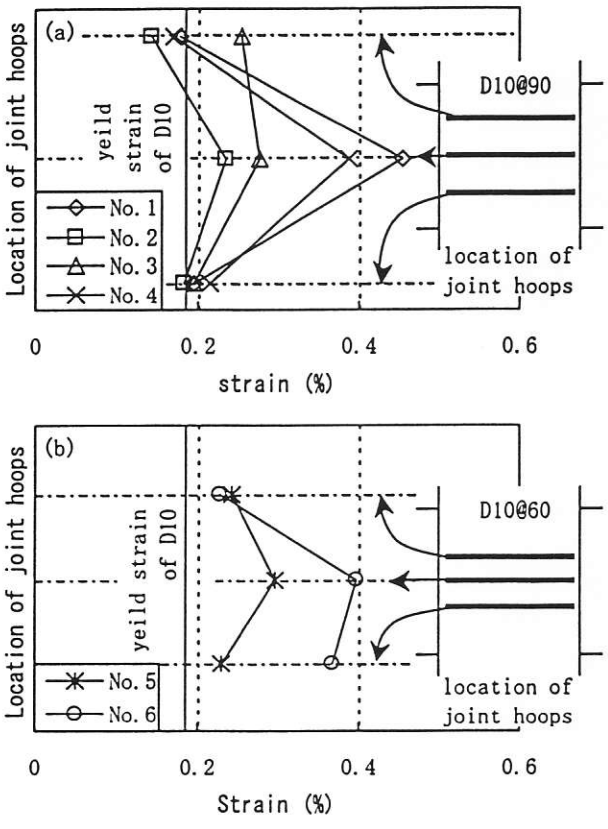

Fig. 4 Strain distributions of joint lateral reinforcemnt

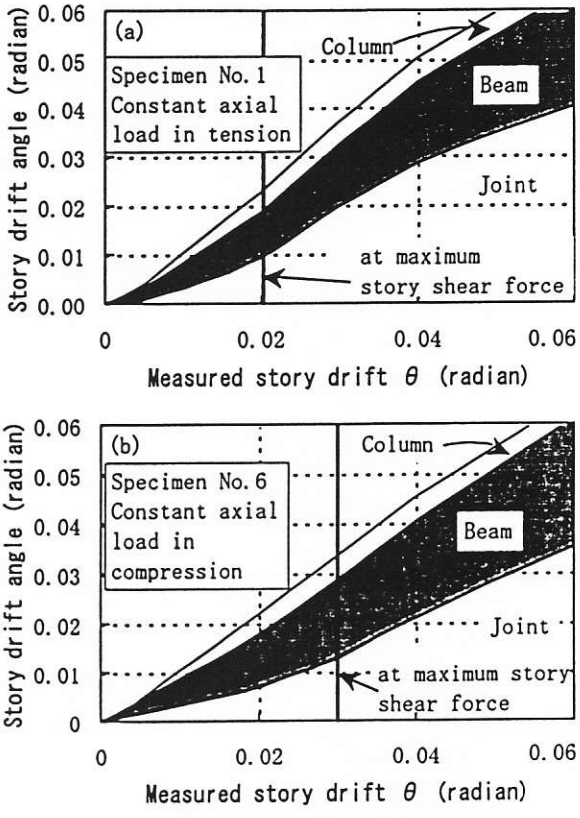

Fig. 5 Components of story drift

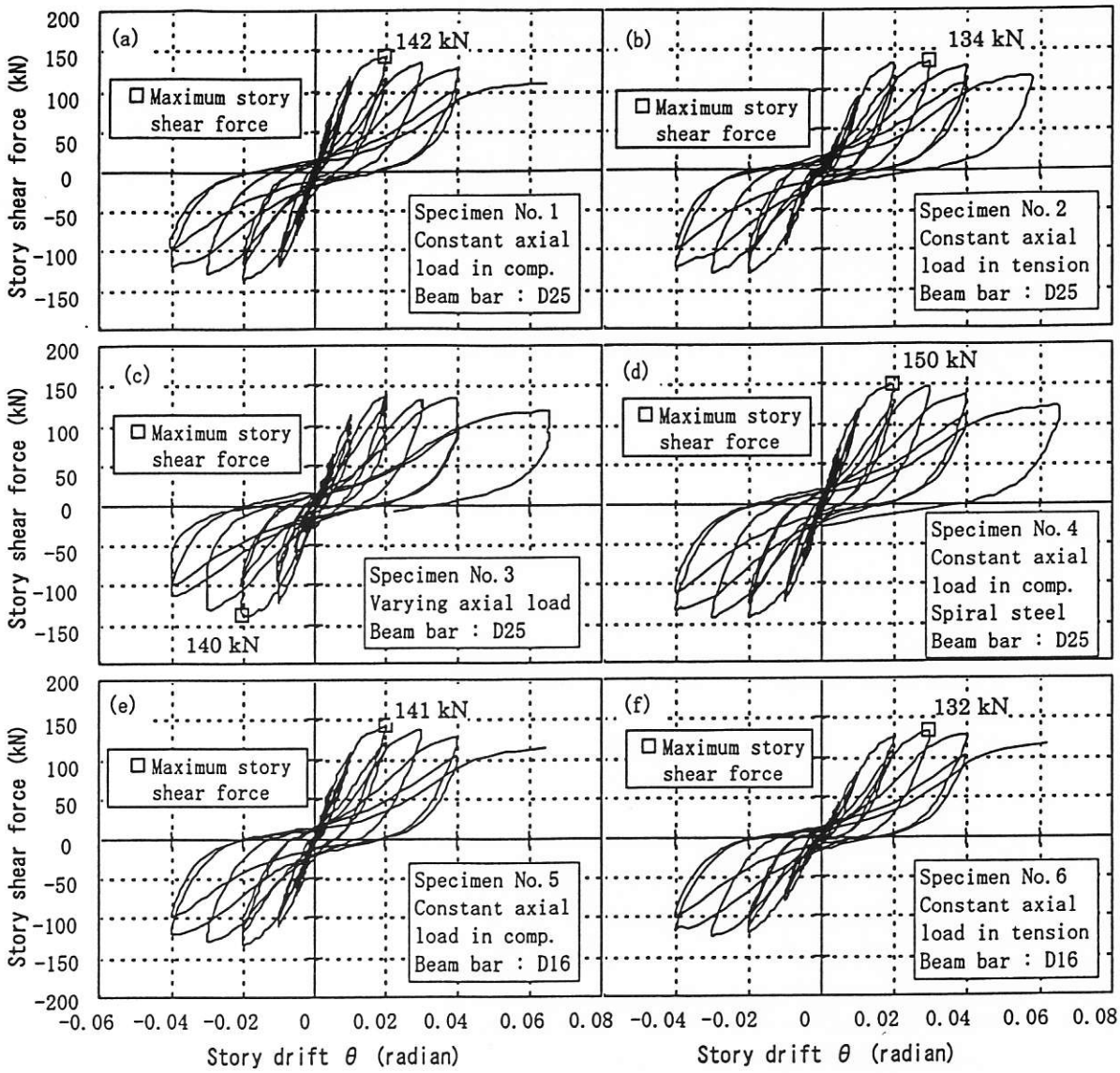

Fig. 6 Story shear force – story drift relationships

the joint panel for the specimens subjected to the compressive column axial load. More diagonal cracks occurred in the joint panel for Specimen No.3 under tensile column axial load than compressive column axial load. The stress of a few beam and column bars yielded at the story drift angle of 1/25 radian for all specimens. Therefore it was judged that the beam and column did not yield. The strain distributions of the joint lateral reinforcement at the maximum story shear force are shown in Fig.4. These strains exceeded the yield strain at the maximum story shear force for all specimens. The contributions of the beam and column deflections and the joint shear distortion to the story drift are shown in Fig.5 for Specimens No.1 and 6. The deflection of beams and columns shared approximately from 60 to 90 % of the total story drift before the maximum story shear force. However, the contribution of the joint shear distortion became large and exceeded the half of the total story drift after the maximum story shear force. Therefore, all specimens eventually failed in joint shear regardless of the column axial load and the beam bar bond condition.

3.2 STORY SHEAR FORCE – DRIFT RELATIONSHIPS

The story shear force – drift relationships are shown in Fig.6. The initial stiffness of Specimen No.1 subjected to the constant column axial load in compression with the beam bar diameter of D25 was larger

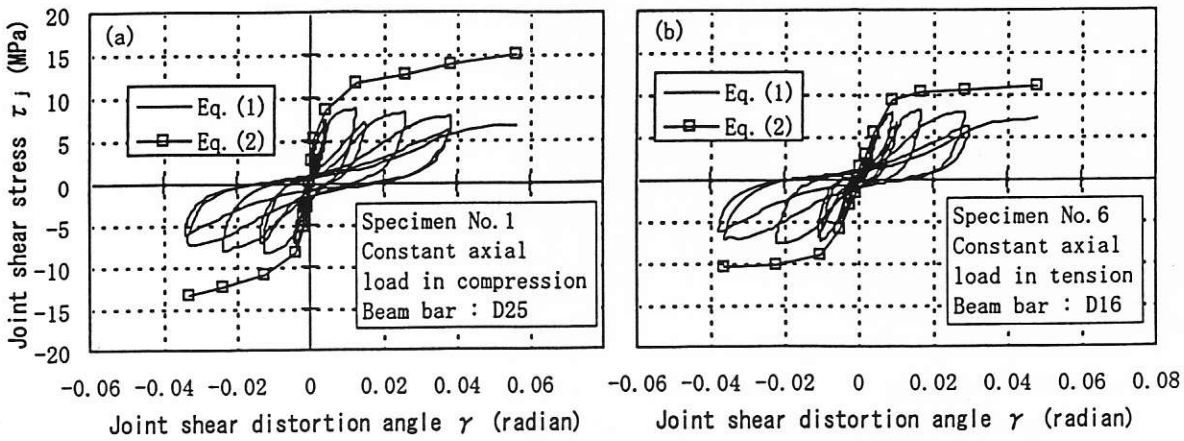

Fig. 7 Joint shear stress - joint shear distortion relationships

than that of Specimen No.2 subjected to the constant column axial load in tension, which was caused by the increase of the bending moment on columns under the compressive column axial load. The story shear force of Specimen No.2 subjected to the constant column axial load in tension with the beam bar diameter of D25 decreased to 0.94 times that of Specimen No.1. The story drift at the maximum story shear force of Specimen No.2 was larger than that of Specimen No.1. The specimens subjected to the constant column axial loads in compression or tension with the beam bar diameter of D16 (called Specimens No.5 and 6) had the same hysteresis characteristics as specimens using the beam bar diameter of D25. Therefore it was judged that the column axial load influenced both the hysteresis characteristics and the story shear strength for beam-column subassemblages. The hysteresis characteristics were almost similar independently of the beam bar diameter among the specimens subjected to the same column axial load. The maximum story shear force of Specimen No.4 that had the beam longitudinal bars reinforced by the spiral steels within a joint was larger than that of another specimens. However the difference among the maximum story shears was little. The influences of different beam bar diameters on the hysteresis characteristics were not observed. The estimation of the story shear capacity at the joint shear strength computed according to the provisions by Architectural Institute of Japan[2] was conservative to the measured story shear for all specimens.

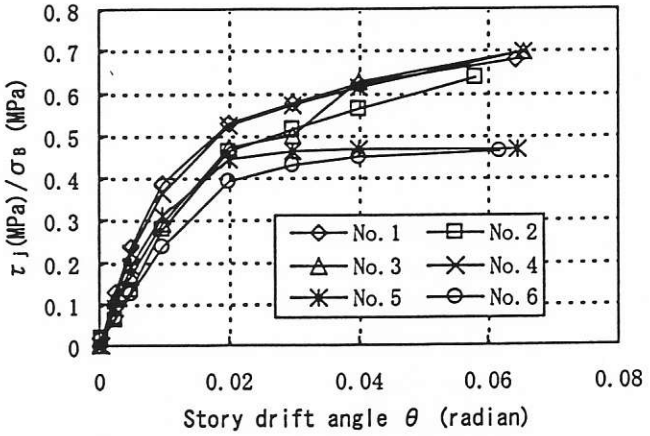

Fig. 8 Normalized joint shear stress - story drift relationships

4. DISCUSSION OF TEST RESULTS

4.1 JOINT SHEAR FORCE – DRIFT RELATIONSHIPS

The joint shear force was computed in two manners mentioned below. a) The tensile force of the beam bars was computed by dividing the beam bending moment on the critical section by a constant lever arm length. The joint shear force is obtained by following equation.

$$V_j = \frac{M_b}{j_b} + \frac{M_b'}{j_b'} - V_c \qquad (1)$$

where M_b and M_b' are beam bending moments on the critical sections, j_b and j_b' are lever arm lengths on the beam critical section and V_c is the measured story shear force. j_b and j_b' are the constant value of 7/8 times

to effective depth of the beam section. b) The tensile force of the beam bars was computed directly from the beam bar strain measured by strain gauges at the critical section. The joint shear force is obtained by following equation.

$$V_j = \Sigma a_t \sigma_s + \Sigma a_t' \sigma_s' - V_c \qquad (2)$$

where a_t and a_t' are the sectional areas of the top and bottom beam bar, σ_s and σ_s' are the stresses of the beam bar on the critical section computed by the measured strains through Ramberg-Osgood Model. The joint shear stresses of Specimens No.1 and 6 from Eqs.(1) and (2) are shown in Fig.7. The joint shear stresses were computed by dividing the joint shear force by the effective sectional area of the joint panel that was the product of the average width of the column and beam multiplied by the column depth. The skeleton curve was shown for the joint shear force computed by Eq.(2). Eq.(1) had been used in general. The joint shear stresses obtained by Eq.(1) decreased after the peak of the story shear force. On the contrary, the joint shear stresses obtained by Eq.(2) increased to the end of the test. The relationships between the joint shear stresses from Eq.(2) normalized by a concrete compressive strength, σ_B, and the story drift angles at peaks of each cycle are shown in Fig.8. Since the joint shear stresses increased successively for all specimens, the decrease in the story shear force is not attributed to the joint shear.

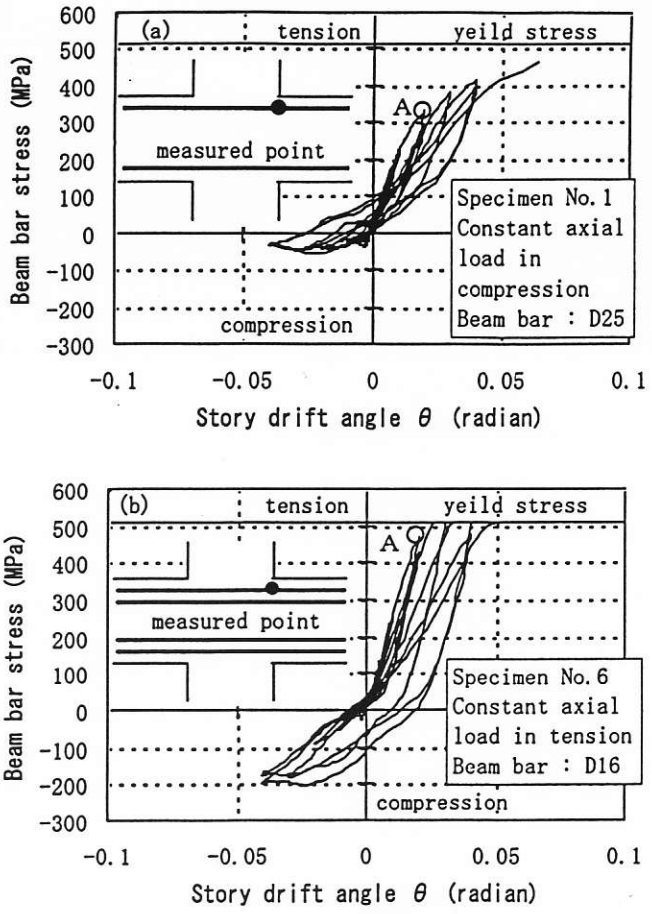

Fig. 9 Beam bar stress - story drift relationships

4.2 BEAM BAR BOND

The beam bar stress – story drift angle relationships for Specimens No.1 and 6 are shown in Fig.9. The bond stresses along a beam bar within a beam-column joint for all specimens are shown in Fig.10. The average bond stress along the beam bars within a joint was computed by the difference of the beam bar

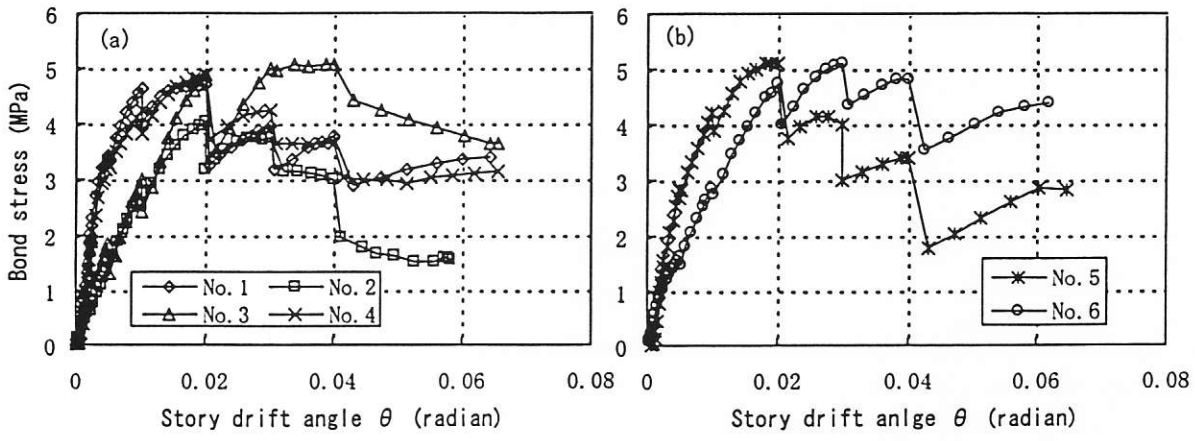

Fig. 10 Bond stress along beam bar within joint - story drift relationships

forces at the opposite column faces. The beam bar diameters little influenced the beam bar bond stress before the story drift angle of approximately 1/50 radian. The bond stresses of specimens subjected to the compressive column axial load were larger than those of the specimens subjected to the tensile column axial load. The bond stress along the beam reinforcement within a joint decreased after the stress reached the bond strength although the tensile force in beam bars at the beam critical section increased successively. Then it was judged that the bond deterioration along beam bars occurred within a joint.

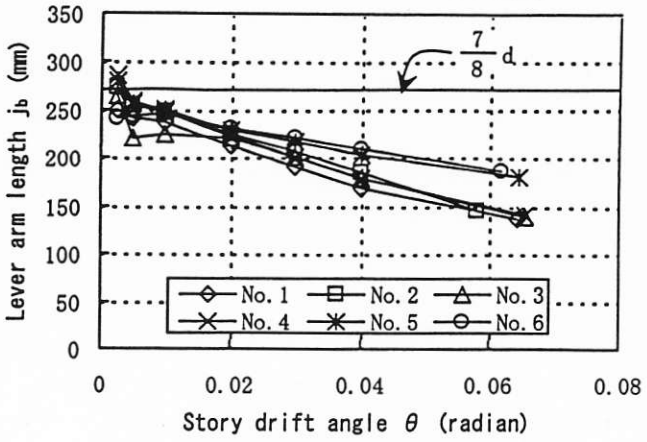

Fig. 11 Change of lever arm length

4.3 LEVER ARM LENGTH

The bond deterioration along beam bars within a joint caused the increase in the compressive resultant force on the beam critical section. Then this made the lever arm length of coupled forces decrease on the beam critical section. The change of lever arm length on the beam critical section is shown in Fig.11. The lever arm length, j_b, was computed by dividing the beam bending moment on the critical section by the tensile force of the beam bars. The lever arm length had a tendency to decrease from 7/8d (d: effective depth of a beam section) for all specimens. The stiffness in the beam bar stress – strain relation decreased suddenly at the point A as shown in Fig.9 while the tensile force of beam bars increased to the end of the test. Therefore the decrease in the bending moment on the beam critical sections resulted in the decay of the story shear force.

4.4 PRINCIPAL STRAIN IN JOINT PANEL

The tensile principal strain – compressive principal strain relationships are shown in Fig.12. The direction of the compressive principal strain to the beam axis for Specimens No.1 and 6 are shown in Fig.13. The principal strains in the joint panel were computed by using average strains measured by two horizontal, vertical and diagonal displacement transducers respectively. The compressive and tensile principal strains increased with the progress of cyclic loading. The stiffness of the joint shear force obtained by Eq.(2) decreased remarkably in the joint shear force – drift relationships as shown in Fig.7. The joint shear distortion increased abruptly because of the increase in the principal strains. The compressive principal strain exceeded the strain of 0.23% at the concrete compressive strength. Therefore the joint failed in a shear through the compressive collapse of the diagonal concrete strut formed in the joint panel. The diagonal joint shear however could be carried by the surrounding concrete of the diagonal strut failed by the compression as shown in Fig.14. This is the

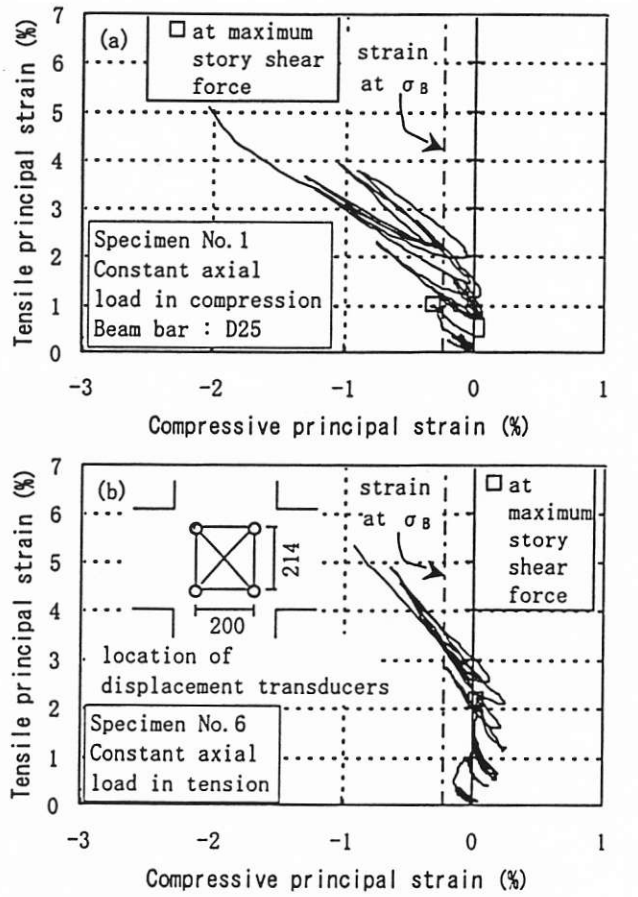

Fig. 12 Tensile prinsipal strain – compressive principal strain relationships

reason why the joint shear does not decrease though the joint fails in a shear. The direction of compressive principal strain increased with the progress of cyclic loading, and reached eventually approximately 60 degrees.

5. CONCLUSIONS

The conclusions obtained in this study can be summarized as follows.

1) The column axial load influenced the story shear strength for beam-column subassemblages. The estimation of the story shear capacity at the joint shear strength computed according to the provisions by Architectural Institute of Japan[2] was conservative to the measured story shear for all specimens.

2) The joint shear obtained by Eq.(2) increased to the end of the test while the story shear force decreased after the maximum story shear force. The tensile force of beam bars increased to the end of the test. Therefore the decrease in the beam bar bond stress within a joint was caused by the bond deterioration.

3) The stiffness of tensile beam bar stress decreased suddenly at the point A as shown in Fig.9 while the lever arm length on beam critical section decreased in proportion to the story shear drift. Therefore the decrease in the bending moment on the beam critical sections resulted in the decay of the story shear force.

4) The stiffness of joint shear force obtained by Eq.(2) decreased remarkably in the joint shear force – drift relationships. The joint shear distortion increased abruptly because of the increase in the principal strains. The joint shear could be carried by the surrounding concrete of the diagonal strut failed by the compression. This is the reason why the joint shear does not decrease though the joint fails in a shear.

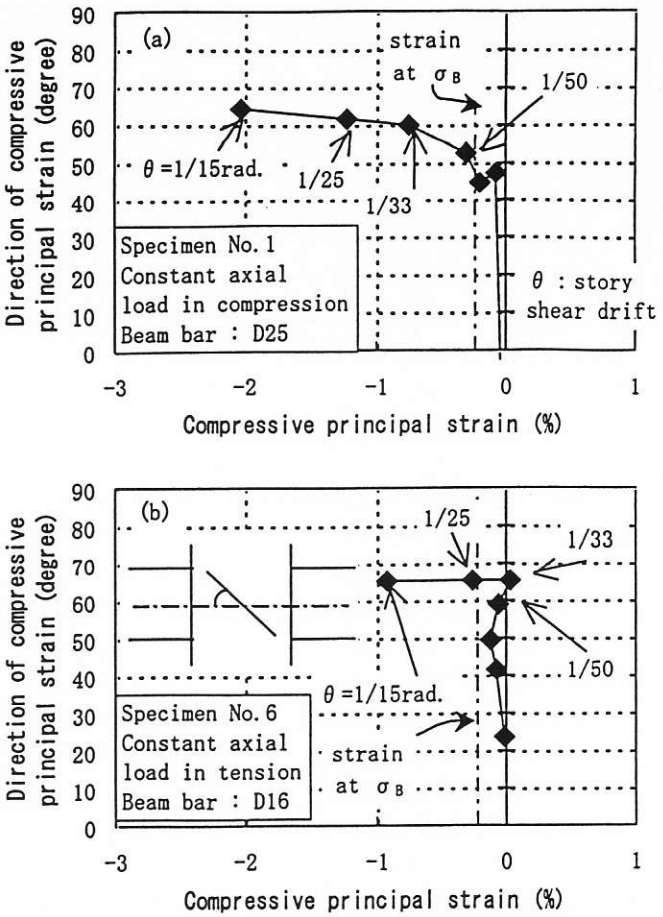

Fig. 13 Direction of compressive principal strain

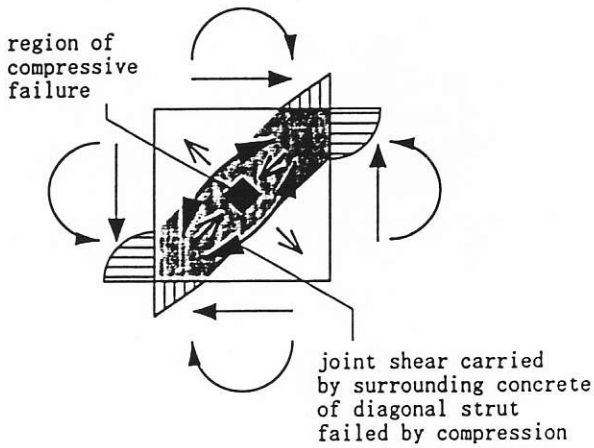

Fig. 14 Stress transmission in joint panel

REFERENCES

(1) Shiohara,H. and F.Kusuhara, "Re-evaluation of Joint Shear Tests of R/C Beam-Column Joints Failed in Shear," Proceedings of the Japan Concrete Institute, Vol.19, No.2, pp.1005-1010, 1997, (in Japanese).
(2) Architectural Institute of Japan, "Design Guidelines for Earthquake Resistant Reinforced Concrete Buildings Based on Inelastic Displacement Concept (Draft)," 1997.